Quantum Mechanical Rate Constants for $H + O_2 \leftrightarrow O + OH$ and $H + O_2 \rightarrow HO_2$ Reactions†

Shi Ying Lin,‡ Edward J. Rackham,§ and Hua Guo*,‡

Department of Chemistry, University of New Mexico, Albuquerque, New Mexico 87131, and Physical and Theoretical Chemistry Laboratory, Oxford University, South Park Road, Oxford, OX1 3QZ, U.K.

Received: June 29, 2005; In Final Form: August 4, 2005

Canonical rate constants for both the forward and reverse $H + O_2 \leftrightarrow O + OH$ reactions were calculated using a quantum wave packet-based statistical model on the DMBE IV potential energy surface of Varandas and co-workers. For these bimolecular reactions, the results show reasonably good agreement with available experimental and theoretical data up to 1500 K. In addition, the capture rate for the $H + O_2 \rightarrow HO_2$ addition reaction at the high-pressure limit was obtained on the same potential using a time-independent quantum capture method. Excellent agreement with experimental and quasi-classical trajectory results was obtained except for at very low temperatures, where a reaction threshold was found and attributed to the centrifugal barrier of the orbital motion.

I. Introduction

The bimolecular reaction

$$H(^2S) + O_2(^3\Sigma_g^-) \underset{k_{-1}}{\overset{k_1}{\leftrightarrow}} O(^3P) + OH(^2\Pi) \qquad (R1)$$

plays a central role in combustion and atmospheric chemistry. The forward reaction is considered to be *the single most important reaction* in the combustion of H_2 and hydrocarbons,[1,2] responsible for the rate-limiting chain-branching ignition and to a large extent for the consumption of oxygen. The reverse reaction is also believed to be involved in many astrochemical[3] and atmospheric processes.[4]

The potential energy surface (PES) governing R1 features a deep HO_2 well,[5,6] 2.38 eV lower than the $H + O_2$ dissociation asymptote. As a result, the reactions are susceptible to the influence of long-lived resonances supported by the HO_2 well. In the high pressure limit, these resonances can be efficiently stabilized by third-body collisions to form the stable HO_2 intermediate:

$$H(^2S) + O_2(^3\Sigma_g^-) \xrightarrow{k_2} HO_2(\tilde{X}^2A'') \qquad (R2)$$

which competes with R1. The HO_2 radical itself has been shown to play an important role in combustion as a possible chain-terminating step. In addition, it is an important intermediate in several gas-phase reactions in the atmosphere. Because of their importance, these reactions have been the subject of extensive experimental[2,7−20] and theoretical investigations.[5,6,21−57] We note that the list is by no means complete and readers are referred to the references cited by these publications. One of the most extensively measured quantities is the canonical rate constant for the $H + O_2 \leftrightarrow O + OH$ reaction over a large temperature range.[14,15,17] Experimental data of the $H + O_2 \rightarrow HO_2$ addition reaction rate at the high-pressure limit has also been reported.[9] Accurate theoretical calculations of these rate constants will provide a stringent test of the PES and detailed knowledge of the reactions themselves.

Since the $H + O_2 \rightarrow O + OH$ reaction is endothermic by 0.71 eV, the threshold for the forward reaction is 3.09 eV above the potential minimum. As a result, the exact quantum mechanical characterization of the $H + O_2 \leftrightarrow O + OH$ reaction is challenging because a large basis/grid is necessary to converge the results in either the time-independent or time-dependent framework. The difficulties are exacerbated by the strong coupling between the helicity substates of the floppy HO_2 species,[31,37,58] rendering the commonly used coupled-state (CS) approximation[59,60] inapplicable. In addition, the reaction is dominated by long-lived resonances supported by the deep HO_2 well,[31,49,51] which can only be resolved with a dense energy grid in the time-independent scattering calculations or by long propagation times.

Because of these difficulties, only a limited number of quantum mechanical (QM) state-to-state reaction probability calculations have thus far been reported for R1 and all were carried out with zero total angular momentum ($J = 0$).[30,31,33,35,43,56,57] Total reaction probabilities have been reported for $J = 0$[34] and for a few nonzero total angular momentum (J) values,[20,36−38] but no rate constant has been derived. Efforts have been made to compute the rate constant directly using the flux correlation function approach, which avoids the state-to-state probabilities. However, these studies also involved approximations such as the CS approximation and J-shifting method for $J > 0$.[44−47] Given the barrierless nature of the reaction, the choice of the barrier, which is necessary for the J-shifting method, can be quite difficult. Similar problems are encountered in a quantum treatment of R2,[29,49−51] and no exact $J > 0$ data have been published.

There have been many quasi-classical trajectory (QCT) studies of both reactions[5,22,23,25,26,42,52,53] Although they provided insightful dynamic information, the accuracy of these results is difficult to establish because the treatment of the zero-point energy and other quantum effects is often dubious.[22,42] This is particularly important for the title reactions because of the

* To whom correspondence should be addressed.
† Part of the special issue "William Hase Festschrift".
‡ University of New Mexico.
§ Oxford University.

10.1021/jp053555v CCC: $33.50
Published on Web 09/08/2005

dominance of threshold effects. In addition to the QCT and QM studies, a number of statistical investigations have been reported for the two reactions,[21,28,40,41,48] but these models typically included no dynamic aspect.

The difficulties associated with an exact QM treatment, namely the involvement of long-lived resonances supported by the deep potential well, paradoxically favor a QM statistical treatment. In the statistical approach,[61−63] the state-to-state reaction probability is completely determined by the probabilities of formation and decomposition of the long-lived intermediate. The long lifetime of the HO_2 resonances near the reaction threshold has been established by theoretical calculations[31,35−37,49,51] and supported by experimental evidence.[19] It should be emphasized that a QM treatment of the complex formation/decomposition processes is necessary, particularly near the reaction threshold, to obtain a reliable characterization of the reactivity. This can be achieved within the statistical model by explicit calculations of the capture probabilities in all arrangement channels, which can be implemented in both time-independent[64,65] and wave packet frameworks.[66] Indeed, recent applications of the statistical model on some complex-forming reactions have enjoyed much success,[64−69] reproducing near-quantitatively the exact results. Encouraged by these successes we applied, in this work, the wave packet based statistical coupled-states method[66] to this important reaction using the popular DMBE IV potential.[5] As discussed in the next section, the large exothermicity in the O + OH → H + O_2 direction renders the capture probability a good approximation for the total reaction probability, at least at low collision energies. The resulting rate constant is related to the rate constant for the reverse reaction via the equilibrium constant, which has been accurately determined experimentally.[8,42] For the H + O_2 addition reaction at the high pressure limit, the capture rate constant was computed using a time-independent coupled-channel approach, which provides an accurate representation of the reaction at very low collision energies. This paper is organized as follows. In the next section (section II), the relevant theoretical methods and their numerical implementations are briefly outlined. In section III, the calculated results are presented and discussed. Finally in section IV, conclusions are made.

II. Theory

For an atom−diatom reaction, the initial state-specified rate constant can be defined as follows:

$$k_i = Q_{\mathrm{el}}^{-1}\sqrt{\frac{8}{\pi\mu(k_{\mathrm{B}}T)^3}}\int_0^\infty \sigma_i(E_{\mathrm{c}})\exp(-E_{\mathrm{c}}/k_{\mathrm{B}}T)E_{\mathrm{c}}\,\mathrm{d}E_{\mathrm{c}} \quad (1)$$

where μ, k_{B}, T, and E_{c} are the translational reduced mass, Boltzmann constant, temperature, and collision energy, respectively. σ_i is the corresponding initial state-specified integral cross-section, obtained by summing either the reaction probabilities for R1 or capture probabilities for R2 over the total angular momentum J. Q_{el} is the electronic partition function. For the H + O_2 → HO_2 addition reaction, $Q_{\mathrm{el}} = 3$.[70] For the O + OH → H + O_2 reaction, on the other hand, the fine-structure of the reactants renders the partition function temperature dependent[27,41]

$$Q_{\mathrm{el}} = [5 + 3\exp(-228/T) + \exp(-327/T)][1 + \exp(-187/T)] \quad (2)$$

where T is in units of Kelvin. The canonical rate constant can be obtained by summing the Boltzmann weighted rate constants for all thermally accessible initial states.

For the O + OH → H + O_2 reaction, initial state-specific reaction probabilities were calculated using a version of the statistical model based on Chebyshev wave packet propagation.[66] A statistical treatment of R1 is justified based on previous observations that the reaction, at low energies, is dominated by narrow resonances which have long lifetimes.[30,31,33] In the statistical approach, the state-to-state reaction probability, $p_{f\leftarrow i}(E)$, is defined as a product of the capture probability in the reactant (i) channel and the fraction of population decaying to the product (f) channel (where i or f collectively denotes particular quantum states in reactant or product channels, respectively):[61]

$$p_{f\leftarrow i}(E) = p_i^{(c)}(E) \times \frac{p_f^{(c)}(E)}{\sum_l p_l^{(c)}(E)} \quad (3)$$

The sum in the denominator of eq 3 runs over all the open channels at energy E. The conserved indices, such as the total angular momentum J and parity are suppressed in eq 3. The capture probabilities can be calculated using either the time-independent close-coupling method[65,71] or wave packet method.[66] In this work, the wave packet method, coupled with the CS approximation, was used since the axis corresponding to that of least moment of inertia coincides reasonably well with the O−OH Jacobi vector.

The calculation of the capture probabilities for all the arrangement channels can be tedious and expensive because there is a very large number of open channels in the H + O_2 asymptote, even near the reaction threshold. This is due to the fact that the H + O_2 asymptote is energetically much lower than the O + OH asymptote and has a much higher density of states than the latter. To obtain the thermal rate constant for O + OH → H + O_2 reaction, however, one only needs to calculate total reaction probabilities which can be approximated as follows:

$$p_i(E) = \sum_f p_{f\leftarrow i}(E) = p_i^{(c)}(E) \times \frac{\sum_f p_f^{(c)}(E)}{\sum_l p_l^{(c)}(E)} \approx p_i^{(c)}(E) \quad (4)$$

The approximation: $\sum_f p_f^{(c)}(E) \approx \sum_l p_l^{(c)}(E)$, which should be valid for the O + OH → H + O_2 reaction at low collision energies, underscores the fact that the reaction R1 is dominated by the dynamics in the O + OH channel. To ensure the validity of the statistical model, the forward rate constant will only be reported here up to 1500 K.

Models similar to eq 4 have been developed by many authors.[40,72] For barrierless reactions leading to a deep well, there is overwhelming evidence supporting the validity of such approaches. Our statistical model is also in spirit similar to the Rice−Ramsperger−Kassel−Marcus (RRKM) theory[73,74] and the statistical adiabatic channel model (SACM).[75] An important difference is that the new model explicitly computes the capture probability using a quantum mechanical method on a realistic PES, thus leading to more reliable results.

Once the rate constant for the reverse direction of R1 (k_{-1}) is known, one can deduce the rate constant for the forward

direction (k_1) via the equilibrium constant

$$K_{eq}(T) = \frac{k_1(T)}{k_{-1}(T)} \tag{5}$$

where the equilibrium constant is given as[8]

$$K_{eq}(T)^{-1} = 2.7 \times 10^{-3} T^{0.4} \exp(8720/T) \tag{6}$$

The recommendation of Troe and Ushakov[42] was not used because its temperature range (1000−5000 K) is higher than what we are interested in this work. Besides, its difference with eq 6 is not significant.

The time-independent close-coupling method,[71] described in earlier work by one of us,[64,65] was used to calculate capture probabilities for reaction R2. The time-independent method was used because it provides an accurate characterization of the reaction at very low collision energies, which is hard to achieve with a wave packet based method because of the difficulties associated with damping outgoing waves with exceedingly long de Broglie wavelengths. We also emphasize that the CS approximation, using the O_2−H distance as the body-fixed quantization axis, was intentionally avoided because of its inaccuracy in this system.[47] (Although choosing the O−O vector as the quantization axis (*r*-embedding[76]) should significantly reduce the coupling between helicity substates in the dissociation asymptote.) In the present work, the reactants were described using Jacobi coordinates, with r and R referring to the O−O internuclear distance and the distance between H and the O_2 center of mass, respectively. Within this framework, the time-independent Schrödinger equation leads to a standard system of coupled equations of the form

$$\psi''(R) = W(R)\psi(R) \tag{7}$$

where the real and symmetric coupling matrix, $W(R)$, may be written as

$$W(R) = \frac{2\mu}{\hbar^2} V(R) + \frac{l(l+1)}{R^2} - k^2 \tag{8}$$

with

$$k^2 = \frac{2\mu}{R^2}(E - \epsilon) \tag{9}$$

Here, μ is the atom−diatom reduced mass, $V(R)$ is a matrix representation of the atom−diatom interaction potential, $\hbar^2 l(l+1)/2\mu R^2$ is a matrix representation of the centrifugal operator, E is the total available energy and ϵ is a diagonal matrix of the diatomic rovibrational energies. It should be noted that due to electronic and nuclear spin symmetry constraints, O_2 is only allowed to populate odd j states,[29] and in the present calculation, not even j functions were included in the basis used to arrive at eq 7.

Capture probabilities for the H + O_2 channel were obtained by solving eq 7 using the log derivative method[77] subject to a capture boundary condition at an inner radius $R = R_c$. As it is not possible to define a quantum mechanical capture initial value, the log derivative matrix, $Y(R) = \psi'(R)\psi(R)^{-1}$, at this inner turning point was obtained using the (multichannel[78]) WKB approximation. Specifically, if $C(R_c)$ is the orthogonal matrix that diagonalizes the coupling matrix at $R = R_c$,

$$\tilde{C}(R_c) W(R_c) C(R_c) = -k(R_c)^2 \tag{10}$$

then the appropriate initial value of $Y(R_c)$ is given by

$$Y(R_c) = -iC(R_c)k(R_c)\tilde{C}(R_c) \tag{11}$$

The log derivative matrix was propagated out to the asymptotic region of the potential where an inelastic scattering matrix, $S(E)$, was obtained using the standard formula,

$$\psi(R) \underset{R\to\infty}{\approx} I_E(R) - O_E(R)S(E) \tag{12}$$

Here, $O_E(R)$ and $I_E(R)$ are diagonal matrices of outgoing and incoming waves,

$$O_E(R) = k^{-1/2} h_l^{(1)}(kR) \tag{13}$$

$$I_E(R) = k^{-1/2} h_l^{(2)}(kR) \tag{14}$$

and $h_l^{(1,2)}(kR)$ are Riccati−Hankel functions.[79]

As pointed out elsewhere,[65] the fact that the log derivative matrix of eq 11 is complex symmetric rather than real symmetric implies that the scattering matrix obtained in such a capture calculation is not unitary. Physically, this lack of unitarity arises from the capture of reactant partners by the collision complex, and it allows us to calculate the capture probability from a given channel c as

$$p_c(E) = 1 - \sum_{c'} |S_{c'c}(E)|^2 \tag{15}$$

where the sum (with index c') runs over all open channels in the Jacobi arrangement of the capture calculation.

The results reported in this work were obtained using the DMBE IV PES of Varandas and co-workers.[5] This PES has a correct description of the long-range interactions, which are vitally important for our calculations. We note in passing that a new PES has recently been developed, and the calculation of the rate constants is reported elsewhere.[80]

III. Results and Discussion

A. H + O_2 ↔ O + OH Reaction. The wave packet-based statistical model[66] was employed to calculate the rate constant for the reverse reaction of R1. As discussed in the previous section, it entails the computation of capture probabilities in the O + OH channel, according to eq 4. The rate constant for the forward reaction of R1 was then obtained indirectly by eq 5. In calculating the capture probabilities, we employed the O−OH Jacobi coordinates (R,r,γ), in which r and R are the O−H internuclear distance and the distance between O and the center of mass of OH, respectively, and γ is the Jacobi angle. The body-fixed z-axis is embedded in R and the electronic-rotational coupling in OH was ignored. As a result, the angular momentum quantum number j (=0, 1, 2, ...) describes rotational states of OH. The Hamiltonian was discretized in a mixed direct product representation. For R and r, the discrete variable representation (DVR) was used,[81] while a finite basis set representation (FBR) was used for the angular coordinate. For R, an equidistant grid was defined in $[R_{min},R_{max}]$ as follows: $R_{\alpha 1} = R_{min} + \alpha_1 \times (R_{max} - R_{min})/(N_R + 1)$ with $\alpha_1 = 1, 2, ..., N_R$, which facilitates a fast sine Fourier transform between the DVR and FBR.[82] For r, on the other hand, N_r potential optimized DVR[83] points were used, which substantially decreased the number of grid points. For the angular dimension, two representations were employed interchangeably. On one hand, the normalized Legendre functions $|j\rangle = \overline{P_j}(\cos\gamma)$ ($j = 0, 1, ..., j_{max}$) were chosen as the basis, and on the other hand, N_γ Gauss−

TABLE 1: Numerical Parameters Used to Calculate Capture Probabilities in the O + OH Channel Using the Wave Packet Method[a]

R_{min}	0.1
R_{max}	20.0
n_R	359
r_{min}	0.7
r_{max}	3.5
n_r	4
j_{max}	24
n_γ	25
R_c	4.1

[a] Atomic units are used.

Legendre quadrature DVR points were defined. A pseudospectral transformation was used to transform between the two representations when needed.[84] The capture radius (R_c), where the flux for complex-forming is calculated, was chosen to be positioned behind the centrifugal barrier. Other details of the calculation can be found in our previous publications.[85−87] Numerical parameters were determined after extensive convergence test calculations, and they are summarized in Table 1. Finally, 20000 steps of Chebyshev propagation[88] were used for capture probability calculations.

As shown in previous work,[64,65] the CS approximation,[59,60] which ignores the Coriolis coupling, is quite accurate in calculating the capture probabilities if the axis of the smallest moment of inertia is close to the atom−diatom axis at long range. Under such circumstances, the accuracy of the CS approximation can be readily understood since the centrifugal barrier is located at relatively large atom−diatom distances where the helicity quantum number (Ω) is often well conserved. This is certainly the case for the O + OH channel, although not so for the H + O_2 channel. The results reported below were thus obtained with the CS Hamiltonian, which is numerically less costly than its exact counterpart including the Coriolis coupling. To obtain the canonical rate constant, calculations have been done for reactant OH initial rotational states from $j_i = 0$ up to $j_i = 15$. The total energy range calculated covers from 0.81 to 1.54 eV, which corresponds to a collision energy range from 0 to 0.73 eV in the case of $j_i = 0$. The maximum total angular momentum $J_{max} = 150$ was found to be sufficient. For $j_i \leq 5$, probabilities for every J were calculated, while for other initial states the probabilities were calculated with an interval of five and the results for the remaining J were interpolated. This method has been tested for $j_i = 0$ case, and found to be very accurate.

In Figure 1, the initial state specified total integral cross sections of the O + OH reaction are displayed for several initial OH rotational states. The cross sections are very large at low collision energies, but they decrease sharply with increasing energy before leveling off. The initial rotational excitation has little effect on the cross section and its energy dependence. In addition, they show no threshold. These features are consistent with the barrierless reaction path leading to a deep potential well.[86,89,90]

By Boltzmann averaging, these total integral cross sections over the collision energy and initial rotational states, the canonical rate constant for the O + OH reaction was obtained and displayed in Figure 2 with several experimental data.[7,8,15,17] Our statistical results are also compared in the figure with the earlier QCT results of Varandas et al.,[25] and QM results of Germann and Miller,[45] who used the flux correlation approach with the J-shifting approximation on the same DMBE IV PES. The calculated rate constant increases first at low temperatures (<80 K) and then decreases at higher temperatures. The irregular

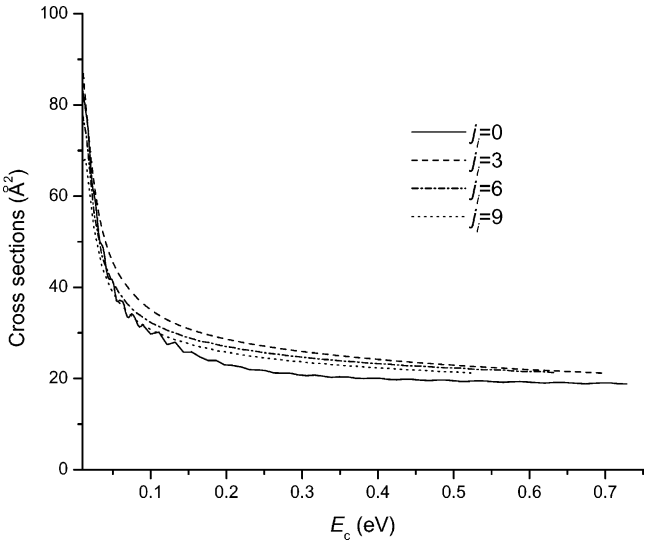

Figure 1. Energy dependence of initial state specified total integral cross sections of the O + OH ($v_i = 0, j_i$) → H + O_2 reaction.

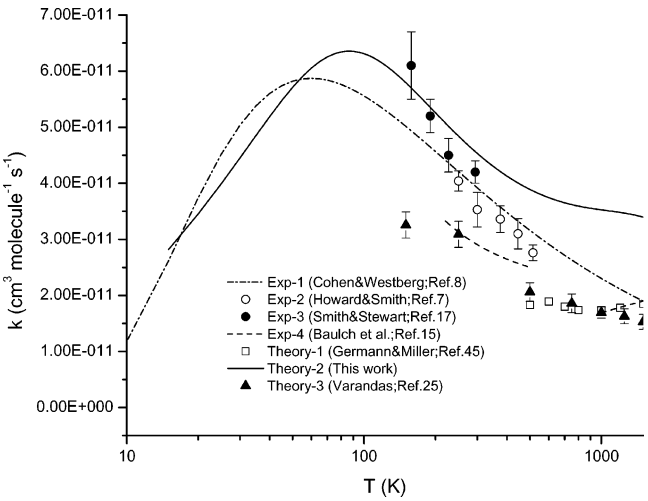

Figure 2. Temperature dependence of canonical (solid line) rate constant for the O + OH → H + O_2 reaction calculated by the statistical model, and comparisons with experimental measurements (Baulch et al.,[15] dashed line; Cohen and Westberg,[8] dash−dotted line; Smith and Stewart,[17] solid circles; Howard and Smith,[7] open circles), QCT results of Varandas et al. (solid triangles),[25] and approximate quantum mechanical results of Germann and Miller (solid squares).[45]

temperature dependence of the rate constant stems largely from the electronic degeneracy factor given by eq 2, and is not a reflection of any specific dynamical behavior. The rate constant obtained from the QM statistical calculation is in excellent agreement with experimental results both in temperature dependence and in absolute magnitude. The deteriorating agreement at high (>400 K) temperatures is expected because the lifetime of the reaction intermediate (HO_2) should decrease as energy increases, and the statistical model becomes inadequate. The statistical rate constant is about a factor of 2 larger than the earlier QM results.[45] The relatively small discrepancy may be due to the failure of the statistical model in this temperature range or to the J-shifting approximation used in the earlier QM work. Our rate constant is also larger than its QCT counterpart,[25] but it is difficult to identify the origin of the discrepancy. Overall, the agreement with both experimental and theoretical data is quite satisfactory.

As stated in the previous section, the canonical rate constant for the forward reaction of R1 was obtained indirectly using eq

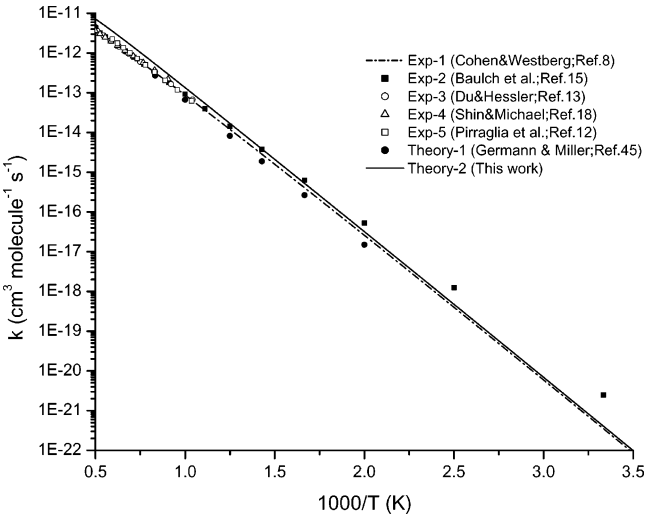

Figure 3. Temperature dependences of canonical rate contant for the $H + O_2 \rightarrow O + OH$ reaction calculated using the statistical model, (this work, solid line) and comparisons with experimental results (Cohen and Westberg,[8] dash−dotted line; Baulch et al.,[15] solid squares; Du and Hessler,[13] open circles; Shin and Michael,[18] open triangles; Pirraglia et al.,[12] open squares) and quantum mechanical result of Germann and Miller[45] (solid circles).

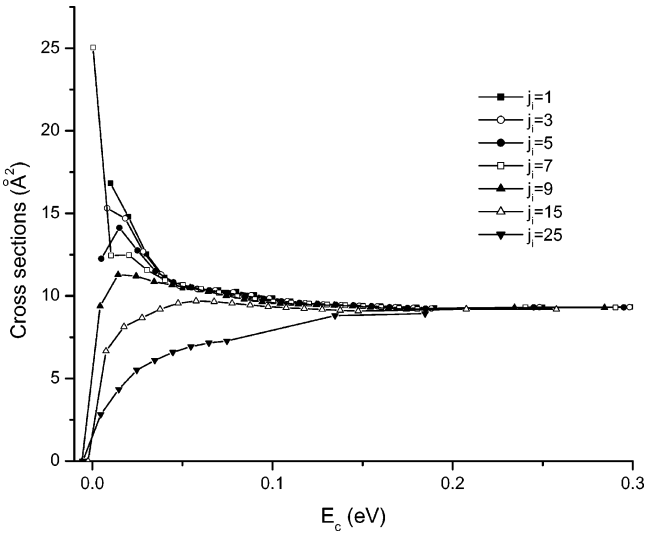

Figure 4. Energy dependence of initial state specified total integral capture cross sections for the $H + O_2$ addition reaction (R2).

5. In Figure 3, the calculated rate constant is compared up to 1500 K with available experimental results[8,12,13,15,18] and with the QM results of Germann and Miller.[45] In keeping with experimental findings, the temperature dependence of the calculated rate constant follows the Arrehnius law, indicated by the linear dependence of the log k with the reciprocal temperature. However, because of the log scale which covers more than 10 orders of magnitude, the agreement between theory and experiment is not as perfect as visually suggested by Figure 3. A closer look, for example, reveals that the statistical results consistently overestimate the experimental data at high temperatures, presumably due to the inadequacies of the statistical treatment of the reaction at high energies. To estimate the theory−experiment discrepancy, the average relative error between the calculated rate constant and the recent experimental data of Baulch et al.[15] was calculated over the 300−1500 K temperature range by sampling at every 5 K. The average error was shown to be 60%. The agreement represents a significant improvement over the previously reported discrepancy of 217 to 304% obtained[28] on the same PES with the phase-space theory, which is essentially a classical version of our statistical model. This improvement underscores the importance of treating the capture process quantum mechanically on a realistic PES. Agreement with the previous quantum results[45,47] is also satisfactory as shown in the figure. Our calculated rate constants at 600 and 1000 K of 5.24×10^{-16} and 1.35×10^{-13} cm^3 molecule^{-1} s^{-1} compare well with the more recent values of 3.39×10^{-16} (4.12×10^{-16}) and 0.90×10^{-13} (1.03×10^{-13}) cm^3 molecule^{-1} s^{-1} reported the Miller group using J-shifting (CS) methods.[47] Interestingly, the rate constant obtained from QCT calculations, 0.99×10^{-13} cm^3 molecule^{-1} s^{-1} at 1000 K,[25] is also in good agreement with our result.

B. $H + O_2 \rightarrow HO_2$ Reaction. Capture probabilities in the $H + O_2$ channel were calculated using a time-independent close coupled method (as discussed in section II) which employed a WKB approximation to the capture initial value. As this semiclassical approximation was used to define the entrance to the collision complex, it was necessary to show that the capture probabilities were well converged with respect to decreasing R_c. (Although this is not the case in general, convergence may be seen with insertion reactions because the local de Broglie wavelength decreases, and thus the semiclassical approximation becomes increasingly justified, as R_c is taken further and further into the deep well region of the potential.) This was found to be the case for $H + O_2$ at a capture radius of $R_c = 3.0\ a_0$. Furthermore, the capture probabilities were unchanged by decreasing R_c by an additional 1.0 a_0. The total energy range calculated covered 0.098 to 0.398 eV leaving a collision energy range of 0.0 to 0.3 eV for $j_i = 1$. For these energies, O_2 states up to and including $j = 39$ were necessary for the calculation and the capture probabilities were found to be nonzero for all J up to $J_{max} = 55$. As mentioned previously, all Coriolis coupling was included exactly in the calculation.

In Figure 4, the energy dependence of the total capture cross section for various O_2 initial states is displayed. The cross sections exhibit sharply different energy dependences at lower energies. For initial states with small j_i, the cross section generally decreases with increasing collision energy, while it rises for those with large j_i. The latter signals a reaction threshold which stems from an entrance channel barrier. Indeed, such a barrier can be identified from the adiabatic potential curves shown in Figure 5. The corresponding barrier is lower than the dissociation threshold for $j_i = 0$, but perks up with nonzero orbital angular momenta. This barrier becomes more conspicuous for large j_i, resulting in the threshold effect seen in Figure 4.

By integration over the collision energy and by the use of thermal averaging over the initial states, the canonical capture rate constant was obtained. The comparison with the QCT results[55] and the available experimental measurement[9] is displayed in Figure 6. The agreement with the experimental rate constant at room temperature is excellent, indicating the overall accuracy of the PES. The agreement with the QCT results is also excellent except for at very low temperatures. The sudden decay of the QM statistical rate constant below 50 K stems from the orbital barrier as discussed above. In QCT calculations, the thermalization of all degrees of freedom allows significant vibrational energy in the O_2 reactant. As the reactants approach each other, energy can leak out of the O_2 vibration to the translational degree of freedom, which might be sufficient to overcome the centrifugal potential barrier. Thus, the discrepancy is likely the result of the lack of proper treatment of the zero-point energy in O_2 in the QCT calculation of the capture rate constant.

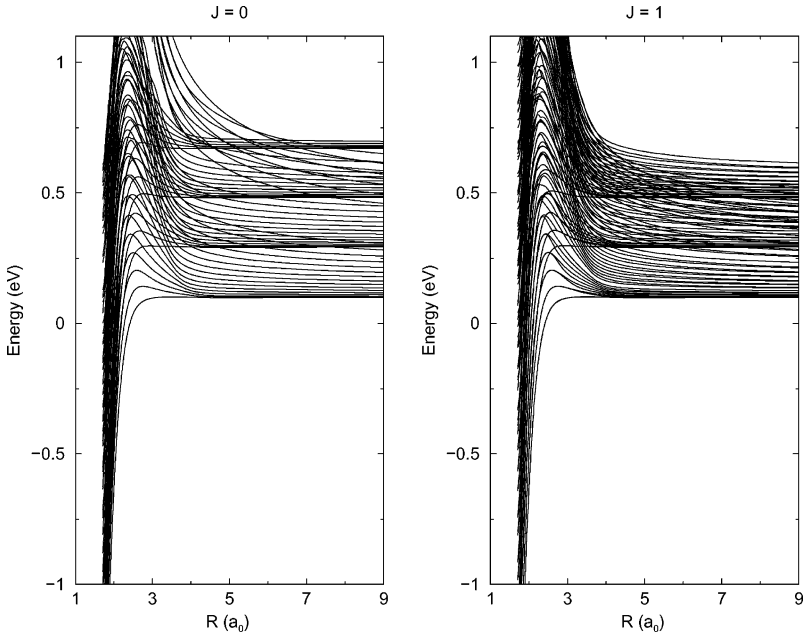

Figure 5. Adiabatic potential curves in the H + O_2 channel for both $J = 0$ and 1 on the DMBE IV PES. The energy is relative to the H + O_2 asymptotic limit.

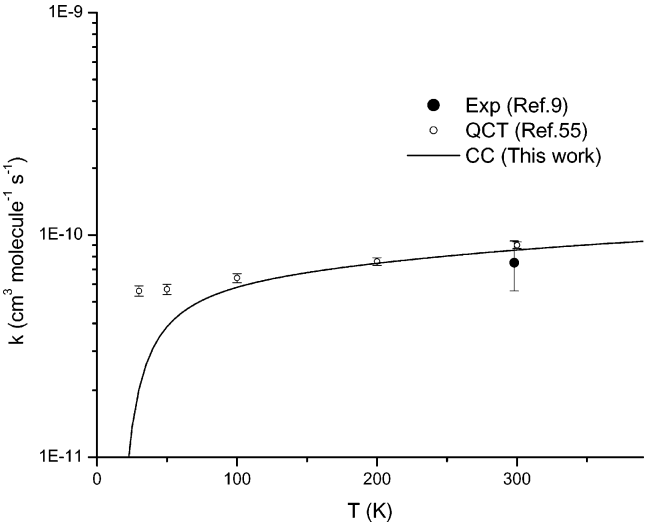

Figure 6. Comparison of quantum and quasiclassical trajectory (QCT)[55] capture rate constants for the H + O_2 addition reaction (R2). The experimental rate constant[9] at 300 K is also included.

IV. Conclusions

In this work, we report quantum mechanical calculations of canonical rate constants for the title reactions, which play a vital role in combustion and in atmospheric chemistry. An accurate representation of the rate constants is essential in kinetic modeling. Calculated rate constants are particularly important when experimental data are not accurate enough to establish a consensus. However, exact quantum mechanical characterization of the rate constant is not trivial even for this triatomic system, primarily because of the large number of quantum states supported by the deep potential well. Here, we take advantage of the long lifetime of the reaction intermediate and use a quantum statistical model to compute the rate constant for the bimolecular reaction. Such a statistical treatment is justified at low collision energies because the reaction is known to be dominated by long-lived resonances. By the same token, the long lifetime of the HO_2 complex is ensured by the high third body collision frequency at the high-pressure limit for the H + O_2 addition reaction.

The calculated canonical rate constants for R1 in both forward and reverse directions are in excellent agreement with available experimental measurements over a wide temperature range up to 1500 K. The agreement with experiment is nearly quantitative for the reverse R1 reaction below 400 K, and ~60% for the forward R1 reaction. This level of success is quite satisfactory, given the drastic approximations assumed in the statistical treatment. For R2, the agreement with both experimental and quasi-classical trajectory results is also very good. At very low temperatures, a reaction threshold has been identified to originate from the centrifugal barrier due to the orbital motion. These results demonstrate again that the statistical model is a powerful tool in studying complex-forming reactions.

Acknowledgment. This work performed at UNM was supported by the National Science Foundation (CHE-0348858). We thank David Manolopoulos and Antonio Varandas for insights and many stimulating discussions. This work is dedicated to Prof. Bill Hase on the occasion of his 60th birthday to honor his numerous scientific contributions and friendship.

References and Notes

(1) Gardiner, W. C. *Combustion Chemistry*; Springer: Berlin, 1984.
(2) Miller, J. A.; Kee, R. J.; Westbrook, C. K. *Annu. Rev. Phys. Chem.* **1990**, *41*, 345.
(3) Viti, S.; Roueff, E.; Hartquist, T. W.; Pineau des Forets, G.; Williams, D. A. *Astron. Astrophys.* **2001**, *370*, 557.
(4) Summers, M. E.; Conway, R. R.; Siskind, D. E.; Stevens, M. H.; Offermann, D.; Riese, M.; Preusse, P.; Strobel, D. F.; Russell, J. M. *Science* **1997**, *277*, 1967.
(5) Pastrana, M. R.; Quintales, L. A. M.; Brandao, J.; Varandas, A. J. C. *J. Phys. Chem.* **1990**, *94*, 8073.
(6) Kendrick, B.; Pack, R. T. *J. Chem. Phys.* **1995**, *102*, 1994.
(7) Howard, M. J.; Smith, I. W. M. *J. Chem. Soc., Faraday Trans. 2* **1981**, *77*, 997.
(8) Cohen, N.; Westberg, K. R. *J. Phys. Chem. Ref. Data* **1983**, *12*, 531.
(9) Cobos, C. J.; Hippler, H.; Troe, J. *J. Phys. Chem.* **1985**, *89*, 342.
(10) Kleinermanns, K.; Wolfrum, J. *Chem. Phys. Lett.* **1984**, *104*, 157.
(11) Bronikowski, M. J.; Zhang, R.; Rakestraw, D. J.; Zare, R. N. *Chem. Phys. Lett.* **1989**, *156*, 7.

(12) Pirraglia, A. N.; Michael, J. V.; Sutherland, J. W.; Klemm, R. B. *J. Phys. Chem.* **1989**, *93*, 282.
(13) Du, H.; Hessler, J. P. *J. Chem. Phys.* **1992**, *96*, 1077.
(14) Baulch, D. L.; Cobos, C. J.; Cox, R. A.; Esser, C.; Frank, P.; Just, T.; Kerr, J. A.; Pilling, M. J.; Troe, J.; Walker, R. W.; Warnatz, J. *J. Phys. Chem. Ref. Data* **1992**, *21*, 411.
(15) Baulch, D. L.; Cobos, C. J.; Cox, R. A.; Frank, P.; Hayman, G.; Just, T.; Kerr, J. A.; Murrells, T.; Pilling, M. J.; Troe, J.; Walker, R. W.; Warnatz, J. *J. Phys. Chem. Ref. Data* **1994**, *23*, 847.
(16) Kim, H. L.; Wickramaaratchi, M. A.; Zheng, X.; Hall, G. E. *J. Chem. Phys.* **1994**, *101*, 2033.
(17) Smith, I. W. M.; Stewart, D. W. A. *J. Chem. Soc., Faraday Trans.* **1994**, *90*, 3221.
(18) Shin, K. S.; Michael, J. V. *J. Chem. Phys.* **1991**, *95*, 262.
(19) Fei, R.; Zheng, X. S.; Hall, G. E. *J. Phys. Chem.* **1997**, *A101*, 2541.
(20) Abu Bajeh, M.; Goldfield, E. M.; Hanf, A.; Kappel, C.; Meijer, A. J. H. M.; Volpp, H.-R.; Wolfrum, J. *J. Phys. Chem.* **2001**, *A105*, 3359.
(21) Rai, S. N.; Truhlar, D. G. *J. Chem. Phys.* **1983**, *79*, 6046.
(22) Miller, J. A. *J. Chem. Phys.* **1986**, *84*, 6170.
(23) Quintales, L. A. M.; Varandas, A. J. C.; Alvarino, J. M. *J. Phys. Chem.* **1988**, *92*, 4552.
(24) Varandas, A. J. C.; Brandao, J.; Quintales, L. A. M. *J. Phys. Chem.* **1988**, *92*, 3732.
(25) Varandas, A. J. C.; Brandao, J.; Pastrana, M. R. *J. Chem. Phys.* **1992**, *96*, 5137.
(26) Varandas, A. J. C. *J. Chem. Phys.* **1993**, *99*, 1076.
(27) Graff, M. M.; Wagner, A. F. *J. Chem. Phys.* **1990**, *92*, 2423.
(28) Yang, C.-Y.; Klippenstein, S. J. *J. Chem. Phys.* **1995**, *103*, 7287.
(29) Kendrick, B.; Pack, R. T. *Chem. Phys. Lett.* **1995**, *235*, 291.
(30) Pack, R. T.; Butcher, E. A.; Parker, G. A. *J. Chem. Phys.* **1993**, *99*, 9310.
(31) Pack, R. T.; Butcher, E. A.; Parker, G. A. *J. Chem. Phys.* **1995**, *102*, 5998.
(32) Kendrick, B.; Pack, R. T. *J. Chem. Phys.* **1996**, *104*, 7502.
(33) Kendrick, B.; Pack, R. T. *J. Chem. Phys.* **1997**, *106*, 3519.
(34) Zhang, D. H.; Zhang, J. Z. H. *J. Chem. Phys.* **1994**, *101*, 3671.
(35) Dai, J.; Zhang, J. Z. H. *J. Phys. Chem.* **1996**, *100*, 6898.
(36) Meijer, A. J. H. M.; Goldfield, E. M. *J. Chem. Phys.* **1998**, *108*, 5404.
(37) Meijer, A. J. H. M.; Goldfield, E. M. *J. Chem. Phys.* **1999**, *110*, 870.
(38) Goldfield, E. M.; Meijer, A. J. H. M. *J. Chem. Phys.* **2000**, *113*, 11055.
(39) Groenenboom, G. C. *J. Chem. Phys.* **1998**, *108*, 5677.
(40) Troe, J. *J. Phys. Chem.* **1986**, *90*, 3485.
(41) Harding, L. B.; Maergoiz, A. I.; Troe, J.; Ushakov, V. G. *J. Chem. Phys.* **2000**, *113*, 11019.
(42) Troe, J.; Ushakov, V. G. *J. Chem. Phys.* **2001**, *115*, 3621.
(43) Sultanov, R. A.; Balakrishnan, N. *J. Phys. Chem.* **2004**, *A108*, 8759.
(44) Leforestier, C.; Miller, W. H. *J. Chem. Phys.* **1994**, *100*, 733.
(45) Germann, T. C.; Miller, W. H. *J. Phys. Chem. A* **1997**, *101*, 6358.
(46) Viel, A.; Leforestier, C.; Miller, W. H. *J. Chem. Phys.* **1998**, *108*, 3489.
(47) Skinner, D. E.; Germann, T. C.; Miller, W. H. *J. Phys. Chem.* **1998**, *A102*, 3828.
(48) Duchovic, R. J.; Pettigrew, J. D.; Welling, B.; Shipchandler, T. *J. Chem. Phys.* **1996**, *105*, 10367.
(49) Mandelshtam, V. A.; Grozdanov, T. P.; Taylor, H. S. *J. Chem. Phys.* **1995**, *103*, 10074.
(50) Mandelshtam, V. A.; Taylor, H. S.; Miller, W. H. *J. Chem. Phys.* **1996**, *105*, 496.
(51) Dobbyn, A.; Stumpf, M.; Keller, H.-M.; Schinke, R. *J. Chem. Phys.* **1996**, *104*, 8357.
(52) Harding, L. B.; Troe, J.; Ushakov, V. G. *Phys. Chem. Chem. Phys.* **2000**, *2*, 631.
(53) Marques, J. M. C.; Varandas, A. J. C. *Phys. Chem. Chem. Phys.* **2001**, *3*, 505.
(54) Harding, L. B.; Troe, J.; Ushakov, V. G. *Phys. Chem. Chem. Phys.* **2001**, *3*, 2630.
(55) Marques, J. M. C.; Varandas, A. J. C. *Phys. Chem. Chem. Phys.* **2001**, *3*, 2632.
(56) Zhang, H.; Smith, S. C. *J. Chem. Phys.* **2002**, *116*, 2354.
(57) Zhang, H.; Smith, S. C. *J. Chem. Phys.* **2002**, *117*, 5174.
(58) Zhang, H.; Smith, S. C. *J. Chem. Phys.* **2003**, *118*, 10042.
(59) McGuire, P.; Kouri, D. J. *J. Chem. Phys.* **1974**, *60*, 2488.
(60) Pack, R. T. *J. Chem. Phys.* **1974**, *60*, 633.
(61) Pechukas, P.; Light, J. C. *J. Chem. Phys.* **1965**, *42*, 3281.
(62) Pechukas, P.; Light, J. C.; Rankin, C. *J. Chem. Phys.* **1966**, *44*, 794.
(63) Miller, W. H. *J. Chem. Phys.* **1970**, *52*, 543.
(64) Rackham, E. J.; Huarte-Larranaga, F.; Manolopoulos, D. E. *Chem. Phys. Lett.* **2001**, *343*, 356.
(65) Rackham, E. J.; Gonzalez-Lezana, T.; Manolopoulos, D. E. *J. Chem. Phys.* **2003**, *119*, 12895.
(66) Lin, S. Y.; Guo, H. *J. Chem. Phys.* **2004**, *120*, 9907.
(67) Alexander, M. H.; Rackham, E. J.; Manolopoulos, D. E. *J. Chem. Phys.* **2004**, *121*, 5221.
(68) Lin, S. Y.; Guo, H. *J. Phys. Chem.* **2004**, *A108*, 10060.
(69) Lin, S. Y.; Guo, H. *J. Chem. Phys.* **2005**, *122*, 074304.
(70) Viel, A.; Leforestier, C. *J. Chem. Phys.* **2000**, *112*, 1212.
(71) Clary, D. C.; Henshaw, J. P. *Faraday Discuss.* **1987**, *84*, 333.
(72) Clary, D. C. *Mol. Phys.* **1984**, *53*, 3.
(73) Marcus, R. A.; Rice, O. K. *J. Phys. Colloid Chem.* **1951**, *55*, 894.
(74) Baer, T.; Hase, W. L. *Unimolecular reaction dynamics, theory and experiments*; Oxford University Press: New York, 1996.
(75) Quack, M.; Troe, J. *Ber. Bunsen-Ges. Phys. Chem.* **1974**, *78*, 240.
(76) Tennyson, J.; Sutcliffe, B. T. *J. Mol. Spectrosc.* **1983**, *101*, 71.
(77) Johnson, B. R. *J. Comput. Phys.* **1973**, *13*, 445.
(78) Johnson, B. R. *Chem. Phys.* **1973**, *2*, 381.
(79) Abramowitz, M.; Stegun, I. A. *Handbook of Mathematical Functions*; Dover: New York, 1970.
(80) Xu, C.; Xie, D.; Zhang, D. H.; Lin, S. Y.; Guo, H. *J. Chem. Phys.* **2005**, *122*, 244305.
(81) Light, J. C.; Carrington, T. *Adv. Chem. Phys.* **2000**, *114*, 263.
(82) Kosloff, D.; Kosloff, R. *J. Comput. Phys.* **1983**, *52*, 35.
(83) Echave, J.; Clary, D. C. *Chem. Phys. Lett.* **1992**, *190*, 225.
(84) Corey, G. C.; Lemoine, D. *J. Chem. Phys.* **1992**, *97*, 4115.
(85) Lin, S. Y.; Guo, H. *J. Chem. Phys.* **2003**, *119*, 11602.
(86) Lin, S. Y.; Guo, H. *J. Phys. Chem.* **2004**, *A108*, 2141.
(87) Lin, S. Y.; Guo, H. *J. Chem. Phys.* **2004**, *121*, 1285.
(88) Chen, R.; Guo, H. *Comput. Phys. Commun.* **1999**, *119*, 19.
(89) Schatz, G. C.; Pederson, L. A.; Kuntz, P. J. *Faraday Discuss.* **1997**, *108*, 357.
(90) Gray, S. K.; Goldfield, E. M.; Schatz, G. C.; Balint-Kurti, G. G. *Phys. Chem. Chem. Phys.* **1999**, *1*, 1141.